

# Analyst

Accepted Manuscript



This is an *Accepted Manuscript*, which has been through the Royal Society of Chemistry peer review process and has been accepted for publication.

*Accepted Manuscripts* are published online shortly after acceptance, before technical editing, formatting and proof reading. Using this free service, authors can make their results available to the community, in citable form, before we publish the edited article. We will replace this *Accepted Manuscript* with the edited and formatted *Advance Article* as soon as it is available.

You can find more information about *Accepted Manuscripts* in the [Information for Authors](#).

Please note that technical editing may introduce minor changes to the text and/or graphics, which may alter content. The journal's standard [Terms & Conditions](#) and the [Ethical guidelines](#) still apply. In no event shall the Royal Society of Chemistry be held responsible for any errors or omissions in this *Accepted Manuscript* or any consequences arising from the use of any information it contains.

Cite this: DOI: 10.1039/c0xx00000x

www.rsc.org/xxxxxx

ARTICLE TYPE

# Non-enzymatic glucose sensing by enhanced Raman spectroscopy on flexible 'as-grown' CVD graphene

Surojit Chattopadhyay,<sup>\*a,b</sup> Mau-Shiun Li,<sup>a</sup> Pradip Kumar Roy,<sup>a</sup> C. T. Wu<sup>c</sup>*Received (in XXX, XXX) Xth XXXXXXXXX 20XX, Accepted Xth XXXXXXXXX 20XX*

DOI: 10.1039/b000000x

Unmodified, as-grown few layer graphene on copper substrates have been used for glucose sensing using Raman spectroscopy. Graphene with stronger 2D band is a better Raman enhancer with significant fluorescence suppression and finer line widths of the Raman signals. The origin of the graphene enhanced Raman spectroscopy (GERS) signal of glucose is attributed to a fractional charge transfer (calculated to be 0.006 using electrochemical parameters) between glucose and graphene aided by a possible  $\pi$ - $\pi$  interaction. Physiological concentrations of glucose (10-500 mg/dl) in PBS have been used for the study. For each glucose concentration, the spectral reproducibility is within 5-25% as calculated by the relative standard deviation of several measurements. The intensity ratio of the 1122  $\text{cm}^{-1}$  peak of glucose and the 2D peak of graphene varied linearly with the glucose concentration and can be used as a calibration curve for unknown sample measurement.

## 1. Introduction

Optical biosensors are in general sensitive, non-invasive and inexpensive and therefore researched with increasing intensity.<sup>1</sup> Blood glucose is one of the earliest molecules whose detection mechanism is quite advanced and mature. Since blood glucose is marker to many of the human diseases, this parameter needs to be checked regularly and easily with high sensitivities keeping the cost to a minimum. Several optical techniques have been used for glucose sensing, such as infrared absorption,<sup>2</sup> laser polarimetry,<sup>3</sup> fluorescence modification of dyes,<sup>4</sup> bioimpedance spectroscopy,<sup>5</sup> and thermal emission spectroscopy.<sup>6</sup> Most of these techniques are not molecule specific and can yield similar results with structurally similar molecules. In this respect Raman spectroscopy is unique, demonstrating molecule-specific vibrational properties. The drawback of a weak scattering cross-section of Raman spectroscopy, compared to fluorescence, could be enhanced by  $10^5$ - $10^{10}$  in the presence of metallic nanoparticles by a method called surface enhanced Raman spectroscopy (SERS).<sup>7</sup> SERS makes use of the internal field of the surface plasmons to electromagnetically enhance the Raman signals from analyte molecules in the vicinity of the metal nanoparticles.<sup>8</sup> For example, Van Duyne and his group did detailed studies of glucose detection using SERS with thiol to adsorb glucose on a silver film coated nanosphere substrate.<sup>9-12</sup> Other SERS studies for glucose sensing also exist but the fabrication of a sensitive biocompatible substrate is a major limiting factor.<sup>13</sup> With the advent of graphene,<sup>14</sup> a highly conducting 2 dimensional (2D) nanomaterial comprising of a single layer of hexagonally arranged carbon atoms, researchers have been trying to use it for SERS.<sup>15</sup> A plasmon resonance, required to enhance the local electric field as in SERS, cannot be excited with a visible laser because it is in the terahertz regime for graphene.<sup>16</sup> It is difficult

to promote even optical absorption in the visible regime as the intrinsic band gap for graphene is very small and neither doping<sup>17</sup> nor structure modification could open up a reasonable band gap. Undaunted by these facts, researchers have used graphene to enhance Raman signals either in conjunction with metal nanoparticles<sup>18,19</sup> or by chemically modifying<sup>20</sup> it to bind to the analyte molecules. Some of these efforts were rewarded with good results, but the select role of graphene was not identified separately. Electrical or electro-chemical approaches to use modified graphene as a sensor material have been carried out with greater success.<sup>21-23</sup> As graphene can be functionalized easily, several biomolecules such as glucose, dopamine, uric acid, ascorbic acid, and others have been detected with unprecedented sensitivity with modified graphene electrochemistry.<sup>22-24</sup> Glucose oxidise modified graphene have been a popular choice among the researches but for electrochemical sensing mostly.<sup>25-27</sup> In short, glucose sensing by graphene, modified or pristine, has been done by electrochemical techniques, and the SERS based sensing studies involved metal nanoparticles only. In this work we have demonstrated that as-grown graphene could be used as a stand-alone enhancer for Raman signals of glucose dissolved in water and PBS in the range of physiologically relevant concentrations. The usability of graphene right out of the CVD furnace into the spectrometric set-up is easier than any other demonstrated optical technique. The issue of sensitivity and reproducibility of the results then just narrows down to a stringent growth condition, and sample screening prior to measurement.

## 2. Results & Discussion

Graphene has been used for molecular sensing in different ways including electrical and optical methods.<sup>28-30</sup> In spite of its applicability in the area of sensing, graphene has an inherent

problem in the microscale domain structure<sup>31</sup> where individual domains are electrically or optically different. This can be due to the presence of varied uncontrolled defects, difference in layer numbers, and edge structures.<sup>32</sup> The difficulty in obtaining optically or electrically equivalent large area graphene is the main reason for the poor reproducibility of results observed in sensing. The TEM image of the graphene samples prepared under low (20

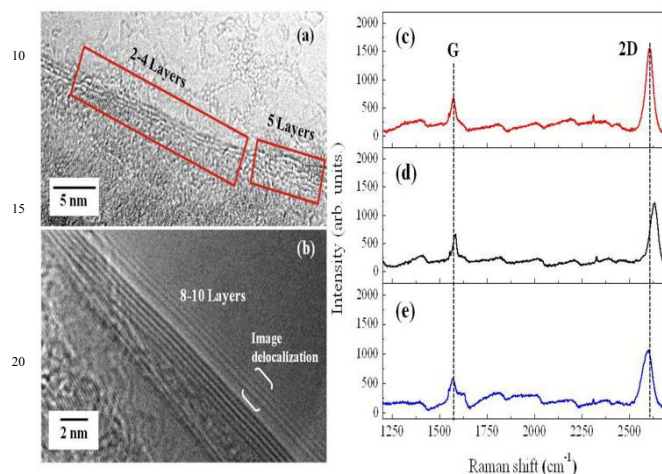


Fig. 1 Representative TEM images of (a) few layer (2-5 layer in this case), and (b) multilayer (8-10 layer in this case) graphene, produced under low (20 sccm) and high (40 sccm) methane flow rates, respectively. Graphene domains with 2-4 layers and 5 layers are marked by the boxes. Note the image delocalization in (b) marked by the bracket. Raman spectra of graphene samples produced with (c) 20, (d) 30, and (e) 40 sccm of methane flow rate. The G and 2D band positions are marked with the dashed vertical lines.

sccm) and high (40 sccm)  $\text{CH}_4$  flow rates are shown in Fig. 1a, and b, respectively. Evidently, the graphene grown with lower  $\text{CH}_4$  flow rate demonstrated fewer layers than those grown under higher  $\text{CH}_4$  flow rates. The sample prepared with 20 and 40 sccm  $\text{CH}_4$  showed 2-5 layer, and 8-10 layer graphene, respectively (Fig. 1a,b). The TEM image in Fig. 1b may suggest 10-15 layer numbers. But actually there are image delocalization effects from the field emission gun as marked by the bracket. Obtaining large area uniform domains with consistent electro-optical properties is difficult and requires higher degree of growth control.<sup>33</sup> One way of checking the graphene quality is measuring the intensity (I) ratio of the 2D and graphitic (G) signal of graphene,  $I_{2D}/I_G$ , using Raman spectroscopy. Generally, the  $I_{2D}$  band intensity increases with lowering of layer numbers.<sup>34,35</sup> The TEM result is corroborated from the Raman measurements shown in Fig. 1 (c-e). The Raman spectra shows clear graphitic (G) bands and the graphene signature 2D bands in all the three samples produced with 20 (Fig. 1c), 30 (Fig. 1d) and 40 sccm (Fig. 1e) of  $\text{CH}_4$ . The lower  $\text{CH}_4$  flow rates, say 20 sccm, yielded few layer graphene structures (Fig. 1c) with stronger  $I_{2D}/I_G$ . Graphene grown with higher  $\text{CH}_4$  flow rates, say 40 sccm, generally yielded a multi-layered structure with lower  $I_{2D}/I_G$  (Fig. 1e). Exact prediction of graphene layer numbers from the  $I_{2D}/I_G$  ratio is difficult without the knowledge of the graphene stacking (turbostratic or AB Bernal).<sup>35</sup> In addition to this, the 2D band

showed phonon stiffening with increasing layer numbers which has been reported before.<sup>36</sup> Although this is a general ensemble feature, reproducibility errors may arise due to the quality of domains actually being excited during the Raman measurements. The other question to answer here is the effect of the domain quality, in other words the  $I_{2D}$ , on the sensing behavior of graphene. To answer this question we performed Raman measurements of glucose by dispersing a known concentration of aqueous glucose solution on these as-grown graphene (Fig. 2). First, only a standard physiological concentration of glucose, 80 mg/dl in water, was dispersed on the three graphene samples as discussed in Fig. 1. Graphene prepared with 20 sccm  $\text{CH}_4$ , having

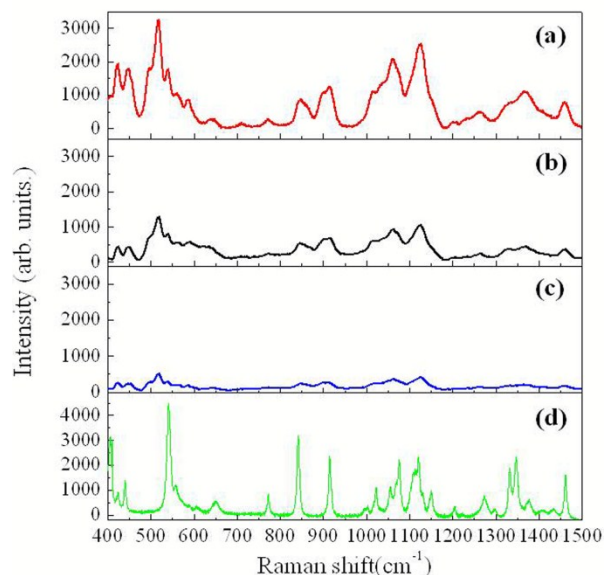


Fig. 2 Graphene enhanced Raman spectra (GERS) of 80 mg/dl glucose solution (in water) dispersed on as-grown graphene produced with (a) 20, (b) 30, and (c) 40 sccm of methane. (d) Raman spectrum of bulk glucose powder dispersed on copper for reference.

a stronger  $I_{2D}$ , showed stronger Raman bands of glucose with significant fluorescence quenching (Fig. 2a) compared to those on graphene produced with 30 and 40 sccm of  $\text{CH}_4$  (Fig. 2b,c) having weaker  $I_{2D}$ . Unlike SERS enhancement obtained with noble metal nanoparticles with a resonance in the visible spectrum, these glucose signal intensities (Fig. 2), measured with a visible laser, did not gain from the graphene plasmon resonance which is in the THz.<sup>16</sup> The Raman signal from the bulk glucose powder was however strong and well resolved even on pure copper (Fig. 2d). The other distinctive feature is that, the Raman spectra of glucose measured on graphene showed clear softening of the major bands compared to that of the bulk glucose powder. The phonon softening ranged from 2-10  $\text{cm}^{-1}$  for the stronger glucose bands observed on the graphene samples. These features are representative only, and depending on the non-uniformity of the quality of the graphene domains there will be certain deviations.

In comparison to the bulk glucose spectrum (Fig. 2d), the signal from even the best graphene (Fig. 2a) does not compare favourably in terms of line width or background subtracted intensity. This is because the number of glucose molecules

optically excited in the bulk sample is far more than that in the 80 mg/dl solution dispersed on graphene. Another reason for the comparatively weaker Raman signals from graphene is the fact that the enhancement expressed therein is not electromagnetic in nature as observed in presence of metal nanoparticles in SERS.<sup>37</sup> A stronger local electromagnetic field accounts for about  $10^6$  and the charge transfer effect accounts for about  $10^2$  enhancement of the Raman scattering cross-section in SERS.<sup>37</sup> The GERS signals obtained from these experiments of glucose on graphene indicates that the charge transfer effect may be predominant in graphene that instead of stepping up the signal intensity quenches the fluorescence from the analyte molecule.

The experimental procedures for Raman measurement are shown schematically in Fig. 3a and b. The procedure is fast and simple and can be performed in less than 10 minutes of sample unloading from the TCVD chamber. The same copper, used as the substrate for graphene growth, has been used as a control (Fig. 3b). Researchers have generally transferred as-grown

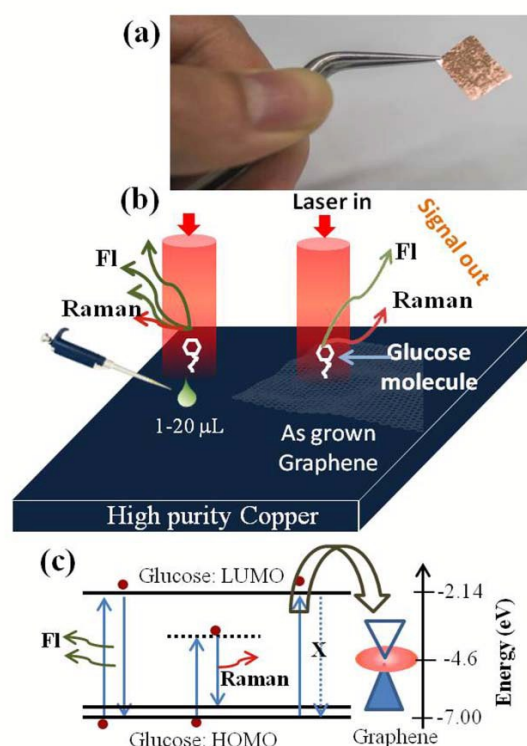


Fig. 3 (a) Photograph of a piece of as-grown graphene on high purity copper foil. (b) A schematic representation of the easy experimental procedure starting with glucose solution dispersion, drying, followed by Raman spectroscopy on copper and graphene using a 632 nm laser. (c) Possible mechanism for high fluorescence (FI) in copper, and fluorescence quenching and Raman enhancement in graphene is described schematically using charge (•) transfer between glucose lowest unoccupied molecular orbital (LUMO at -2.14 eV) and Fermi energy of graphene at -4.6 eV. The horizontal dashed line in (c) show virtual excited states for Raman scattering in glucose.

graphene (on copper) to silica substrates for better adhesion or electrical insulation. However, as our technique is optical,

electrical insulation is not an issue. The extra step of graphene transfer, using quality degrading corrosive chemicals, is time consuming and hence avoided here. Optically, the as-grown graphene is as pristine as experimentally possible (Fig. 3a,b). A schematic mechanism for the fluorescence quenching from glucose on graphene is schematically depicted in Fig. 3c.

Having optimized the graphene prepared with 20 sccm  $\text{CH}_4$ , we have carried out concentration dependent Raman spectroscopy of glucose in this sample compared to that on a pure copper foil as reference. Fig. 4 compares the Raman spectra of glucose on plain copper (Fig. 4 a-e), and on copper supported graphene (Fig. 4 g-k). 510, and 1122  $\text{cm}^{-1}$  bands are signatures for glucose.<sup>9-12</sup> A closer evaluation of the concentration dependent spectra reveals finer line width, and better band clarity, indicating stronger fluorescence suppression in the GERS data compared to those on copper. This result in better spectral resolution but limited signal intensity which is consistent with the lower enhancement values associated with the charge transfer theory of SERS.<sup>18,33</sup> However,

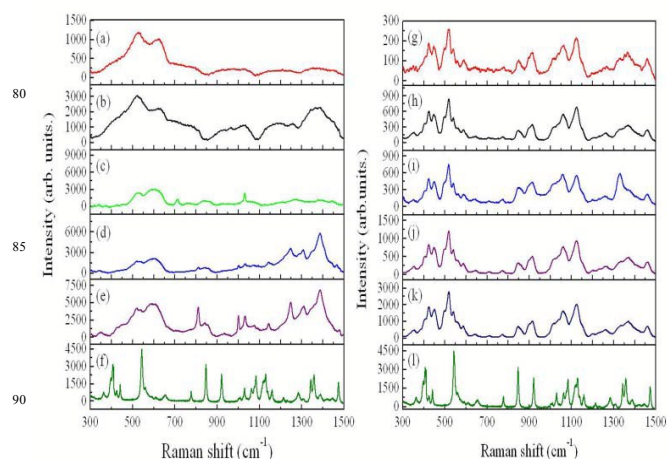


Fig. 4 Baseline corrected Raman spectra of glucose solution (in water) with concentrations of (a) 10, (b) 50, (c) 80, (d) 150, (e) 200 mg/dl, and (f) bulk glucose powder dispersed on copper substrate. Graphene enhanced Raman spectra of glucose solution (in water) with concentrations of (g) 10, (h) 50, (i) 80, (j) 150, (k) 200 mg/dl, and (l) bulk glucose powder dispersed on as-grown graphene (on copper) substrate.

bulk glucose still showed stronger and significantly well resolved Raman bands of glucose (Fig. 4f, l).

Sugars such as glucose, fructose, and sucrose all have Raman bands with specific fingerprint spectra. The loss of specificity in the disaccharide spectrum, say sucrose – a combination of glucose and fructose, resembling those of the monosaccharides, can be solved using statistical models (such as PLS) and procedures.<sup>38</sup> However, the 1122  $\text{cm}^{-1}$  peak that we have used to identify glucose is specific. Fig. S1† shows the variation of the intensity of the two major bands of glucose, namely, the 1122 and the 510  $\text{cm}^{-1}$  bands, as a function of the glucose concentration, measured on graphene. Although the variation is linear within 150 mg/dl of glucose concentration, the 200 mg/dl concentration signal was clearly much stronger than the other concentrations. This is consistent for both the 1122 (Fig. S1a†), and 510  $\text{cm}^{-1}$  (Fig. S1b†) glucose bands as measured on graphene. The attempted linear fit of the data yielded low correlation

coefficients below 0.9.

To understand the GERS signal reproducibility on graphene, Raman measurements were performed at different spots on the same sample. Different concentrations of glucose solution (10-500 mg/dl), made in PBS to better mimic the physiological conditions, were dispersed on optimized graphene. The Raman intensities as a function of concentration were as expected, but showed reproducibility problems. To quantify the reproducibility we calculated the statistical relative standard deviation ( $RSD = \text{standard deviation}/\text{mean}$ ). The RSD ranged between 5-25% for the samples studied (bottom plot in each panel of Fig. 5). The RSD decreased at higher glucose concentrations. This may be attributed to the better glucose molecule coverage on the excited graphene substrate. At lower glucose concentrations (10-80 mg/dl), with lower and non uniform sample surface coverage, the RSD increased. This is corroborated by the fact that the samples with lower glucose concentrations showed stronger  $I_{2D}$  graphene band compared to analyte signals. For better control on the measurement and analysis, the wetting property (hydrophobicity or hydrophilicity) of graphene may have to be considered in future studies. For measurements with real blood samples, ultracentrifugation and further preparation is required to separate and discard the cellular part whose large size would suppress any optical enhancement from the underlying graphene.

The adsorption of glucose on the graphene network and the charge transfer mechanism may be facilitated by the similar

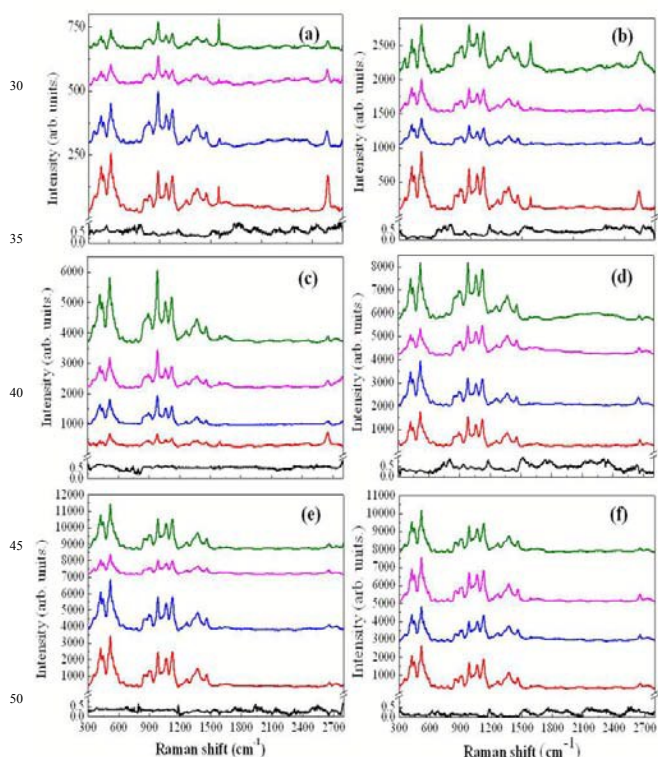


Fig. 5 Concentration dependent GERS spectra of glucose (in PBS) collected from 4 different spots of the same graphene sample (a) 10, (b) 50, (c) 200, (d) 300, (e) 400, and (f) 500 mg/dl. The relative standard deviation (RSD) of the four spectra are presented by the black line at the bottom of each panel.

hexagonal carbon ring structure expressed in graphene and glucose. The stacking of glucose on graphene may be as a result of the  $\pi$ - $\pi$  interaction.<sup>39</sup> For glucose, the carbonyl, dominating the lowest unoccupied molecular orbital (LUMO) is the site where optically excited electron will be accommodated. However, the presence of larger p-orbitals in graphene, will also attract the electron for reaction. The highest occupied molecular orbital (HOMO) and LUMO in glucose dictates the ionization potential ( $I_p$ ), and the electron affinity ( $A$ ), respectively. The difference in the electronegativities ( $X$ ) of glucose and graphene will drive the electron transfer ( $\Delta n$ ) from glucose to graphene. This reaction may also result in the ring formation. These quantities have been calculated<sup>40,41</sup> and shown in Table-I assuming these definitions still hold in a zero bandgap graphene.

Table 1 Calculation of ionization potential, electron affinity, electronegativity, electrochemical hardness and softness, electrophilicity index, and fractional charge transfer in the glucose-graphene system.

Material	$I_p = -E_{\text{HOMO}}$ (eV)	$A = -E_{\text{LUMO}}$ (eV)	$X = (I_p + A)/2$	$\eta = (I_p - A)/2$	$\sigma = 1/\eta$	$\omega = X^2/2\eta$	$\Delta n = \frac{(X_{\text{graphene}} - X_{\text{glucose}})}{2(\eta_{\text{graphene}} + \eta_{\text{glucose}})}$
Glucose	7.00	2.14	4.57	2.43	0.41	4.29	0.006
Graphene	4.6	4.6	4.6	0	-	-	-0.006

where  $I_p$  = Ionization potential;  $A$  = electron affinity;  $X$  = electronegativity;  $\eta$  = hardness;  $\sigma$  = softness;  $\omega$  = electrophilicity index;  $\Delta n$  = fraction of electron transfer.

Such interactions have been reported on molecules having the hexagonal carbon ring structures.<sup>23, 24, 28</sup> This interaction provides a pathway for electron transfer between the LUMO of glucose at -2.14 eV and the Fermi energy of graphene at -4.6 eV (Fig. 3c). The calculated electron transfer fraction<sup>41</sup> of 0.006 (Table I) will reduce the spontaneous fluorescence from the analyte molecule, glucose, as observed in the GERS results (Fig. 3c, Fig. 4 g-k). There is a report stating that the charge transfer occurs predominantly at the first layer in graphene, and that molecular adsorption at the first layer is critical for the signals generated.<sup>42</sup> Another supporting report by Xie *et al.*<sup>43</sup> claims three orders of magnitude reduction in the fluorescence scattering cross-section by graphene. Some quantities in Table I, such as  $\sigma$ , and  $\omega$  for graphene that theoretically tends to infinity because  $\eta=0$ , are kept blank to underline the fact that these values have not been reported experimentally for graphene. The negative sign for  $\Delta n$  of graphene (Table I) implies electron accepting property of graphene when interacting with glucose. In addition to the  $\pi$ - $\pi$  interaction, other adsorption mechanisms cannot be ruled out. Kong *et al.*<sup>39</sup> revealed the influence of defects in graphene to enhance the Raman signals from pyridine by density functional theory.

Such a charge transfer should reveal itself in the shift of the G-band of graphene.<sup>44</sup> We did observe such a shift of the G band from 1575  $\text{cm}^{-1}$  in pristine graphene to 1595  $\text{cm}^{-1}$  in graphene dispersed with 200 mg/ml glucose (Fig. S2†). However, beyond 200 mg/dl, we did not see further shift of the G-band. This may be due to significant screening of the graphene domains from the incident laser by the deposited glucose molecules which we believe to be multilayered at such high concentrations. We have

shown previously, that charge transfer is limited and it's rate is slower as analyte adsorption exceeds a monolayer configuration on graphene electrodes used for electrochemical sensing.<sup>45</sup>

Lastly, a calibration curve needs to be generated to measure unknown glucose concentrations from Raman measurements. As Fig. S1† did not yield a linear variation over the 10-200 mg/dl glucose concentration because of the artefacts responsible for the RSD as mentioned above, an alternative strategy has to be proposed. Here, we have normalized the GERS signals of glucose, say the 1122 cm<sup>-1</sup> line intensity, with the I<sub>2D</sub> of graphene, and found that the reproducibility problem due to optically different graphene domains could be partly resolved. Fig. 6 shows the variation of the Raman signal intensity ratio I<sub>1122</sub>/I<sub>2D</sub> as a function of the glucose concentration in the range 10-500 mg/dl. In this case we obtained a better fit to the data with an acceptable correlation coefficient of 0.95. This data set can be used as a calibration curve for glucose sensing using as-grown graphene. A sensitivity of 0.02 counts/mg/dl could be obtained using the presented formalism. The rationale behind such normalization is as follows: the Raman signal (say I<sub>1122</sub>) from glucose is proportional to the glucose concentration and is also dependent on the I<sub>2D</sub> of graphene in an unknown manner. Therefore, I<sub>1122</sub>/I<sub>2D</sub> should be concentration dependent only, assuming uniform surface coverage of the analyte at all concentrations. However, confirmation from other works using other analytes is necessary. Critically speaking, optimization and uniformity in graphene quality is an issue for the sensing purpose. Graphene uniformity will ensure similar 2D peak intensity for the measurements and hence a better linearity of the signal in the span of the concentration used. In this case, the non-uniformity in the sample domains gave rise to different I<sub>2D</sub> and resulted in a higher RSD. The increase in the analyte signal with the graphene I<sub>2D</sub> is unknown. Hence, when normalizing with graphene I<sub>2D</sub> the slope of the calibration curve may not be high, but if ensured sample uniformity (same I<sub>2D</sub>) the sensitivity would be high and consistent. This is why sample uniformity and repeatability is critical for a real device fabrication.

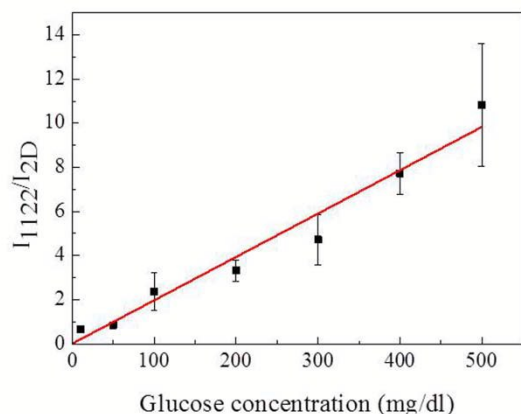


Fig. 6 Variation of the ratio of the intensities of the 1122 cm<sup>-1</sup> Raman line of glucose and the 2D Raman line of graphene as a function of glucose (in PBS) concentration. The line joining the data points is a linear fit to the data with an acceptable correlation coefficient of 0.95.

### 3. Experimental

In this work, graphene films, of about 5 cm<sup>2</sup>, were grown on 0.25mm thick high purity copper foil substrates from Alfa Aesar by thermal chemical vapour deposition (TCVD) using hydrogen (H<sub>2</sub>), methane (CH<sub>4</sub>), and argon mixture as gaseous precursors. The as-purchased copper foil was sandwiched between two glass slides and pressed tightly with alligator clamps and left to flatten. A small cut was made in the lower right corner of the foil for positional reference later on. Before insertion into the quartz furnace, the copper foil was cleaned by dipping it in the Acetone for 10 minutes. The loading of the copper foil is done with the help of a ceramic boat. The Cu-foil was heated in Ar (50 sccm) at 200 mTorr pressure to 950 °C for 35 minutes. The temperature was held constant over the next 30 minutes. H<sub>2</sub> and CH<sub>4</sub> were introduced at 1050 °C at times of 65 and 105 min, respectively. The growth processes were performed at 1000°C, at low pressures (200 mTorr). The graphene growth continued for 15 min at 500 mTorr pressure and stopped by turning off the CH<sub>4</sub>, with conventional radiation cooling to room temperature. Strong air blowing was employed to ensure fast cooling of the sample. Graphene samples thus prepared were analyzed by Raman spectroscopy with the aim to assess their quality and fine tune the growth process. At and around the optimized conditions continuous films consisting of very few graphene layers could be produced reproducibly. The Raman and Graphene enhanced Raman Spectroscopy measurements were done using a commercial Jobin Yvon LabRAM HR800 (HORIBA Ltd.) Raman spectrometer equipped with an Olympus BX-41 microscope, using 632 nm laser excitation (beam diameter ~2µm, power 10 mW, exposure time 5 sec, 3 accumulations). The spectral resolution of the machine was 1 cm<sup>-1</sup>. For GERS measurements, 10.0 µL of either aqueous or PBS solution of glucose, standard alpha-D (+)-Glucose (99+%, Acros, Belgium), was used for the study.

Glucose solution in deionized (DI) water or phosphate buffer solution (PBS) was then dispersed on the graphene surface using a pipette in a measured way (10 µL). The sample was then dried in a rotary vacuumed dry box in room temperature and taken for Raman measurements.

Transmission electron microscopy (TEM) of the graphene samples were done using a FEI Tecnai F20 operated at 200 kV.

### 4. Conclusion

As-grown graphene on copper substrates, without any functionalization or modification, have been used for glucose sensing using Raman spectroscopy. Few layer graphene with stronger 2D band showed better analyte signals compared to the multi-layered graphene. 10-200 mg/dl glucose in water and 10-500 mg/dl glucose in PBS have been used for the study. Graphene resulted in a suppression of the fluorescence and better resolution of the glucose peaks in Raman spectroscopy with weak intensity enhancement. The origin of the enhanced Raman signals of glucose on graphene is attributed a fractional charge transfer, calculated at 0.006 using published electrochemical data, from

glucose to graphene aided by a possible  $\pi$ - $\pi$  interaction. The phenomenon is therefore called graphene enhanced Raman spectroscopy (GERS). The intensity ratio of the 1122  $\text{cm}^{-1}$  peak of glucose and the 2D peak of graphene varied linearly with the glucose concentration and can be used as a calibration curve for unknown sample measurement. The sensing measurement reproducibility is within 5-25% which could be improved with stringent and uniform sample selection.

## 5. Acknowledgements

This work has been carried out with financial assistance from National Science Council (MOST-101-2112-M-010-003-MY3), Taiwan.

## Notes and references

- <sup>15</sup> <sup>a</sup> Institute of Biophotonics, National Yang-Ming University, 155 Sec-2, Li-Nong Street, Taipei-112, Taiwan.  
E-mail: [sur@ym.edu.tw](mailto:sur@ym.edu.tw)  
Tel.: +886 2 2826 7909// Fax: +886 2 2823 5460
- <sup>20</sup> <sup>b</sup> Biophotonics and Molecular Imaging Research Centre, National Yang Ming University, Taipei-112, Taiwan.
- <sup>25</sup> <sup>c</sup> Nano Device Materials Characterization Division, National Nano Device Laboratories, Hsinchu-300, Taiwan.
- <sup>28</sup> † **Electronic Supplementary Information (ESI) available** : Calibration curve showing variation of  $I_{510}$  and  $I_{1122}$  as a function of glucose concentration. See DOI: 10.1039/b000000x/
- 1 R. J. McNichols and G. L. Cote', *J. Biomed. Opt.*, 2000, **5**, 5–16.
  - 2 R. D. Rosenthal, L. N. Paynter and L. H. Mackie, US Patent No. 5,028,787, 1991.
  - 3 W. March, R. Engerman and B. Rabinovitch, *ASAIQ Trans.*, 1979, **25**, 28–31.
  - 4 J. R. Lakowicz and B. Maliwal, *Anal. Chim. Acta*, 1993, **271**, 155–164.
  - 5 A. Caduff, E. Hirt, Y. Feldman and H. L. Ali, *Biosens. Bioelectron.*, 2003, **19**, 209–217.
  - 6 J. M. Buchert, *Proceedings of the SPIE*, 2004, **5566**, 100–111.
  - 7 S. Chattopadhyay, H. C. Lo, C. H. Hsu, L. C. Chen and K. H. Chen, *Chem. Mater.*, 2005, **17**, 553–559.
  - 8 Y. F. Huang, C.Y. Chen, L. C. Chen, K. H. Chen and S. Chattopadhyay, *NPG Asia Materials*, 2014, **6**, e123.
  - 9 K. E. Shafer-Peltier, C. L. Haynes, M. R. Glucksberg and R. P. Van Duyne, *J Am Chem Soc.*, 2003, **125**, 588–593.
  - 10 C. R. Yonzon, C. L. Haynes, X. Y. Zhang, J. T. Walsh and R. P. Van Duyne, *Anal. Chem.*, 2004, **76**, 78–85.
  - 11 D. A. Stuart, C. R. Yonzon, X. Zhang, O. Lyandres, N. C. Shah, M. R. Glucksberg, J. T. Walsh and R. P. Van Duyne, *Anal. Chem.*, 2005, **77**, 4013–4019.
  - 12 J. M. Yuen, N. C. Shah, J. T. Walsh, M. R. Glucksberg and R. P. Van Duyne, *Anal. Chem.*, 2010, **82**, 8382–8385.
  - 13 O. Lyandres, J. M. Yuen, N. C. Shah, R. P. Van Duyne, J. T. Walsh, Jr. and M. R. Glucksberg, *Diabetes Tech. Ther.*, 2008, **10**, 257–265.
  - 14 K. S. Novoselov, A. K. Geim, S. V. Morozov, D. Jiang, Y. Zhang, S. V. Dubonos, I. V. Grigorieva and A. A. Firsov, *Science*, 2004, **306**, 666–669.
  - 15 W. Xu, N. Mao and J. Zhang, *Small*, 2013, **9**, 1206–1224.
  - 16 L. Ju, B. Geng, J. Horng, C. Girit, M. Martin, Z. Hao, H. A. Bechtel, X. Liang, A. Zettl, Y. R. Shen and F. Wang, *Nat. Nanotech.*, 2011, **6**, 630–634.
  - 17 H. Liu, Y. Liu and D. Zhu, *J. Mater. Chem.*, 2011, **21**, 3335–3345.
  - 18 F. Schedin, E. Lidorikis, A. Lombardo, V. G. Kravets, A. K. Geim, A. N. Grigorenko, K. S. Novoselov and A. C. Ferrari, *ACS Nano*, 2010, **4**, 5617–5626.
  - 19 W. G. Xu, X. Ling, J. Q. Xiao, M. S. Dresselhaus, J. Kong, H. X. Xu, Z. F. Liu and J. Zhang, *Proc. Natl. Acad. Sci.*, 2012, **109**, 9281–9286.
  - 20 W. Ren, Y. X. Fang and E. K. Wang, *ACS Nano*, 2011, **5**, 6425–6433.
  - 21 Y. Liu, D. Yu, C. Zeng, Z. Miao and L. Dai, *Langmuir*, 2010, **26**, 6158–6160.
  - 22 M. Zhou, Y. Zhai and S. Dong, *Anal. Chem.*, 2009, **81**, 5603–5613.
  - 23 Z. H. Sheng, X. Q. Zheng, J. Y. Xu, W. J. Bao, F. B. Wang and X. H. Xia, *Biosens. Bioelectron.*, 2012, **34**, 125–131.
  - 24 K. J. Huang, Q. S. Jing, Z. W. Wu, L. Wang and C. Y. Wei, *Coll. Surf. B: Biointerfaces*, 2011, **88**, 310–314.
  - 25 B. Unnikrishnan, S. Palanisamy and S.-M. Chen, *Biosens. Bioelectron.*, 2013, **39**, 70–75.
  - 26 X. Kang, J. Wang, H. Wu, I.A. Aksay, J. Liu and Y. Lin, *Biosens. Bioelectron.*, 2009, **25**, 901–905.
  - 27 C. Shan, H. Yang, J. Song, D. Han, A. Ivaska and L. Niu, *Anal. Chem.*, 2009, **81**, 2378–2382.
  - 28 J. Du, R. Yue, F. Ren, Z. Yao, F. Jiang, P. Yang and Y. Du, *Biosens. Bioelectron.*, 2014, **53**, 220–224.
  - 29 Y. H. Kwak, D. S. Choi, Y. N. Kim, H. Kim, D. H. Yoon, S. S. Ahn, J. W. Yang, W. S. Yang and S. Seo, *Bios. Bioelectron.*, 2012, **37**, 82–87.
  - 30 C. Shan, H. Yang, J. Song, D. Han, A. Ivaska, and L. Niu, *Anal. Chem.*, 2009, **81**, 2378–2382.
  - 31 P. Y. Huang, C. S. Ruiz-Vargas, A. M. van der Zande, W. S. Whitney, M. P. Levendorf, J.W. Kevek, S. Garg, J. S. Alden, C. J. Hustedt, Y. Zhu, J. Park, P. L. McEuen and D. A. Muller, *Nature*, 2011, **469**, 389–393.
  - 32 Z. Liu, Y.C. Lin, C.C. Lu, C.H. Yeh, P.W. Chiu, S. Iijima and K. Suenaga, *Nature Comm.*, 2013, **5**, 4055.
  - 33 R. S. Weatherup, C. Baehtz, B. Dlubak, B. C. Bayer, P. R. Kidambi, R. Blume, R. Schloegl and S. Hofmann, *Nano Lett.*, 2013, **13**, 4624–4631.
  - 34 M. S. Hu, C. C. Kuo, C. T. Wu, C.W. Chen, P. K. Ang, K. P. Loh, K. H. Chen and L. C. Chen, *Carbon*, 2011, **49**, 4911–4919.
  - 35 J. S. Hwang, Y. H. Lin, J. Y. Hwang, R. Chang, S. Chattopadhyay, C. J. Chen, P. Chen, H. P. Chiang, T. R. Tsai, L. C. Chen, and K. H. Chen, *Nanotechnol.*, 2013, **24**, 015702.
  - 36 J.S. Park, A. Reina, R. Saito, J. Kong, G. Dresselhaus and M.S. Dresselhaus, *Carbon*, 2009, **47**, 1303–1310.
  - 37 M. Moskovits, *Rev. Mod. Phys.*, 1985, **57**, 783–826.
  - 38 K. Ilaslan, I. Hakki Boyaci, A. Topcu, *Food Control*, 2015, **48**, 56–61.
  - 39 X. K. Kong and Q. W. Chen, *J. Mater. Chem.*, 2012, **22**, 15336–15341.
  - 40 A. Lesar and I. Milošev, *Chem. Phys. Lett.*, 2009, **483**, 198–203.
  - 41 I. Lukovits, E. Kalman and F. Zucchi, *Corrosion*, 2001, **57**, 3–8.
  - 42 X. Ling and J. Zhang, *Small*, 2010, **6**, 2020–2025.
  - 43 L. M. Xie, X. Ling, Y. Fang, J. Zhang and Z. F. Liu, *J. Am. Chem. Soc.*, 2009, **131**, 9890–9891.
  - 44 C.N.R. Rao and R. Voggu, *Materials Today*, 2010, **13**, 34–40.
  - 45 P. K. Roy, A. Ganguly, W.H. Yang, C.T. Wu, J.S. Hwang, Y.Tai, K.H. Chen, L.C. Chen and S.Chattopadhyay, *Biosens. Bioelectron.*, 2015, **70**, 137–144.